CHAPTER 3
GOLD COMPOUNDS: STRUCTURE AND DRUG-LIKENESS

SUMMARY

Background: Drug-likeness characteristics of compounds that are newly synthesised for biological testing or which are part of virtual libraries have to be investigated early in the drug development process. The compounds (twenty seven in total: eight precursors and nineteen complexes) tested in this study were synthesized and characterized by chemists of the Project AuTEK Biomed consortium. The compounds consisted of four gold*(I) phosphine chloride complexes and four complementary ligands, four bis(phosphino) hydrazine (BPH) gold(I) chloride complexes, six gold(I) thiolate complexes, four gold(III) thiosemicarbazonate complexes and corresponding ligands and a gold(III) pyrazolyl complex. These compounds were analysed for stability and similarity to known drugs with regards to chemical structure.

Materials and Methods: ^{31}P and ^{1}H NMR spectra were obtained to determine the stability of representative complexes from each class. Drug-likeness studies were performed using *in silico* prediction models for ADMET and lipophilicity in the Discovery Studio Software package from Accelrys. The *in silico* lipophilicity predictions were compared to those obtained using the traditional shake flask method and to those obtained for available anti-HIV agents.

Results and Discussion: The ^{31}P NMR chemical shifts of a gold(I) phosphine chloride complex (TTC3), and a BPH gold(I) complex (EK231), remained stable after one week analysis dissolved in deuterated (*d6)*-DMSO and stored at -20 ºC and 37 ºC respectively. In the ^{1}H NMR spectra of complexes TTC3, MCZS3, PFK174 and PFK7, a water peak on day zero suggested inherent hygroscopic abilities which became prominent after 24 h and on day 7 (attributable to the hygroscopic nature of DMSO). The water peak appeared to have no discernible effect on structure since the backbone chemical shifts of most of the complexes were maintained but aqueous solubility appeared to be affected especially for complexes MCZS3 and PFK174. Of the nineteen gold complexes analysed, acceptable drug-like properties were predicted for eight and these findings were comparable to those of existing drugs. There was good correlation between experimental (shake flask) and *in silico* lipophilicity prediction values for two of the complexes; thus confirming the *in silico* findings.

Conclusion: Compounds with satisfactory drug-like properties which also demonstrate inhibitory activity (chapter 4 and 5) will be recommended as leads for further testing. Those with poor properties which end up being inhibitory will be recommended for optimisation by structural modification to increase drug-likeness while maintaining or improving potency.

Keywords: Compound structure, drug-likeness, *in silico*, ADMET properties, stability.

*chemical notation does not use space

Various transition metals have been exploited for therapeutic activity and have wide application in medicine ranging from the treatment of arthritis and cancers to microorganism infections (reviewed by Rafique *et al*., 2010). These metal-based drugs which are chemically synthesised complexes containing the relevant metal coordinated to suitable ligands form what is also known as metallodrugs. The metal of interest in this study is gold which is chemically represented as Au. Gold is a transition metal element with an atomic weight of 197 and is a member of group IB on the periodic table. Gold exists in three oxidation states which are gold(0) or metallic gold, gold(I) and gold(III). Gold(III) and gold(I) are easily reduced to gold(0) in the presence of reducing agents and in the absence of stabilizing ligands (Merchant, 1998). Gold(0) is the least active (Merchant, 1998).

The ligands used play a crucial role in the synthesis of gold or metal-based complexes not only because complexation confers stability, but in some cases leads to better activities and/or reduced toxicities (Pelosi *et al*., 2010, Beraldo and Gambino, 2004). Since ligands can be chemically modified to accommodate different functional groups or atoms, a diversity of possibilities with regards to complex types is possible. This diversity is further enhanced by the fact that the d orbital of metals are in the process of filling such that different coordination complexes can be formed (Rafique *et al*., 2010). This is the advantage that inorganic medicinal chemistry has over organic medicinal chemistry (Fricker, 2007) since a diverse number of chemical entities can be synthesised.

Gold-containing complexes are well known for their application as anti-rheumatoid arthritic agents (Champion *et al*., 1990, Fricker, 1996) but also show activity against various microorganisms including HIV (reviewed by Fonteh *et al*., 2010). In this project, the interest in synthesizing new gold-based complexes was not only sparked by the need for identifying novel therapy for the treatment of HIV infection but also by the history of these complexes with regards to anti-HIV activity. The earliest limitation of gold-based complexes that had activity against HIV was the fact that inhibition in direct enzyme assays could not be correlated in cell-based assays. This was because the compounds could not be readily taken up by cells and thus could not reach therapeutic levels to inhibit viral targets within the cell in cultures (Zhang *et al*., 1994). A typical example is the injectable gold(I) thiolate complex, aurothioglucose, which inhibited RT in cell-free assays (Okada *et al*., 1993) but together with its metabolites could not be taken up by cells.

Phosphine-containing ligands have better membrane permeability profiles (Gandin *et al*., 2010). The phosphine complexes screened here which were fourteen in total, included four gold(I) phosphine chloride-based complexes (P-Au-Cl) designated TTC3, TTC10, TTC17 and TTC24, four BPH gold(I) chloride-containing complexes (P-Au-Cl) designated EK207, EK208, EK219 and EK231 and six gold(I) phosphine thiolate-containing complexes (S-Au-P) designated MCZS1, MCZS2, MCZS3, PFK174, PFK189 and PFK190. The sulphur-containing ligand in the S-Au-P complexes is known to readily bind to gold (Abdou *et al*., 2009). This

ease of binding to gold is a property that is displayed during ligand exchange reactions when these compounds interact with sulfhydryl groups in cysteine residues of proteins (Roberts *et al*., 1996, Bernners-Price *et al*., 1996, Allaudeen *et al*., 1985). In the fourteen complexes, the gold atom formed strong covalent bonds with the ligands through coordination with S and P. Covalent bonds formed with S, P and C result in complexes with good stability and longer shelf life (Parish and Cottrill, 1987).

The oxidation state of any metal is a critical factor in considering chemotherapeutic applications (Thompson and Orvig, 2003). Gold(I) complexes are generally preferred because of their stability and because they are less toxic than gold(III). The use of hard donor ligands such as N and O which result in relatively stable gold(III) complexes (Milacic and Dou 2009) has led to the synthesis of more physiologically stable gold(III) complexes. Gold(III) complexes with anti-HIV activity have been reported with their stability linked to the ligand choice (Sun *et al*., 2004). Five of the compounds tested in this study were gold(III) complexes and consisted of four gold(III) thiosemicarbazone-based complexes designated PFK7, PFK8, PFK41 and PFK43 and a gold(III) pyrazolyl complex designated KFK154b. Gold(III) gives rise to complexes that are isoelectric and isostructural like those of platinum (Bruni *et al*., 1999) and have thus been analysed for anti-cancer activity (Gabbiani *et al*., 2007, Messori *et al*, 2004, Che *et al*., 2003, Marcon *et al*., 2002) because of the anti-cancer activity associated with cisplatin (a platinum-based metallodrug). The choice of Tscs as ligands for gold(III) synthesis was not only motivated by the fact that these compounds consist of mixed donor atoms (N,S) that resulted in considerably stable gold(III) complexes. It was also because Tscs-based complexes have previously shown anti-HIV activity (Pelosi *et al.*, 2010, Mishra *et al*., 2002, Pandeya *et al*., 1999) and it was thus envisaged that complexation with gold will enhance this activity as a result of the conferred stabilisation of the compound after complexation.

In summary, the factors that were considered during synthesis (so as to increase the drug-likeness of the complexes) included the compounds' potential for inhibiting HIV, potential for stability in biological media and lipophilic tendencies. Studies in the late 1990s indicated that poor pharmacokinetics and toxicity ranked high among the causes of late-stage failures in drug development (van de Waterbeemd and Gifford, 2003, Lombardo *et al*., 2003). This finding dictated that methods to eliminate non drug-like compounds early in drug discovery were essential. In addition to *in vitro* HTS assays that have been developed to determine drug-likeness, *in silico* computational methods have been emerging as complementary approaches (Desai *et al*., 2006). Besides aiding in optimising the drug discovery process, computational tools also help in the identification of leads from large libraries according to certain restrictions such as ideal lipophilicity values. Here, the use of computational screening (e.g. ADMET predictions) was mainly for optimisation and to complement findings from biological assays as well as to prioritise hits based on drug-likeness.

In *in vitro* HTS assays, the ability to easily retrieve and test compounds is a priority and compounds are typically dissolved in DMSO and stored until needed (Ellson *et al*., 2005). Unfortunately DMSO is highly hygroscopic and easily absorbs water from the atmosphere. In a DMSO solution, water accelerates degradation of compounds and causes precipitation thereby affecting product concentration (Ellson *et al*., 2005). This could lead to problems ranging from underestimated activity, variable data, inaccurate SAR, discrepancies in enzyme and cell-based assays and inaccurate *in vitro* ADMET data (Di and Kerns, 2006). *In vitro* ADMET refers to drug-likeness properties determined in culture (e.g. using caco-2 cells for cellular permeability determination, Egan and Lauri, 2002) unlike *in silico* ADMET which refers to computational predictions. To investigate whether the structural composition of the compounds was still intact (compared to when synthesised) and the effect of solvent on storage and stability, NMR profiles of representative complexes in *d6*-DMSO were obtained. This is because the only information on compound stability that could be obtained from the *in silico* ADMET predictions studies was that of plasma protein binding ability. It was therefore important that stability in the solvent used in dissolving the complexes be determined using the alternative NMR procedure.

In the next sections, the structures and chemical names of the compounds will be provided as well as brief summaries of the synthetic procedures and references to publications and reports containing detailed information on synthesis. Stability and storage issues will then be addressed as well as the ADMET predictions for drug-likeness. This will be followed by information on lipophilicity determination to confirm *in silico* predicted values for two of the complexes using the traditional shake flask method. In addition, the ADMET findings will be compared to the “Lipinski’s rule of five” which states that poor absorption or permeation is more likely when there are > 5 H-bond donors, >10 H-bond acceptors, the molecular weight (Mr) is > 500 and when the calculated log P is > 5 (Lipinski *et al*., 1997). The “five” in the name of the rule does not refer to the number of rules but to the fact that each property is described in multiples of 5. According to the rule, a compound with values which exceed any two of the properties has particularly poor absorption or solubility. “Lipinski’s rule of 5” forms a model that has been widely used for the prediction of passive intestinal absorption (Egan and Lauri, 2002, Lipinski *et al*., 1997).

3.2 COMPOUNDS

The gold complexes that were tested in this study have been grouped according to the ligand types that were used during synthesis. The different ligand structures within and between groups contributed to the diversity of the gold complexes. In some cases the corresponding ligands were also tested as controls to verify the effect of complexation. This was however not possible in all cases because not all the ligands were stable enough for

biological testing as observed and stated by the chemists e.g. the BPH ligands were prone to decomposition even under inert conditions but not upon complexation (Kriel *et al*., 2007).

3.2.1 The Gold(I) Phosphine Chloride-containing Complexes – Class I

The gold(I) phosphine chloride class of compounds consisted of four ligands and four complementary gold(I) phosphine complexes. The ligands are designated TTL3, TTL10, TTL17 and TTL24 while the complementary complexes are represented as TTC3, TTC10, TTC17 and TTC24 respectively. The structures, identification codes and full chemical names are shown in Table 3.1. Synthesis involved the production of ligands starting from commercially available 2-(diphenylphosphino)benzaldehyde (Traut and Williams, 2006). This was followed by complexation of the synthesised phenethyl amine or *N,N*-dimethyl-ethane-1,2-diamine-containing phosphine ligands with (THT)AuCl (where THT=tetrahydrothiophene) as gold starting material (Traut and Williams, 2006, shown in Figure 3.1A and B). Characterisation was then performed using ^{31}P NMR. In all cases, the coordination of the gold to the ligand was by covalent interaction with P. The synthesis and characterization of these compounds has been published (Williams *et al*., 2007).

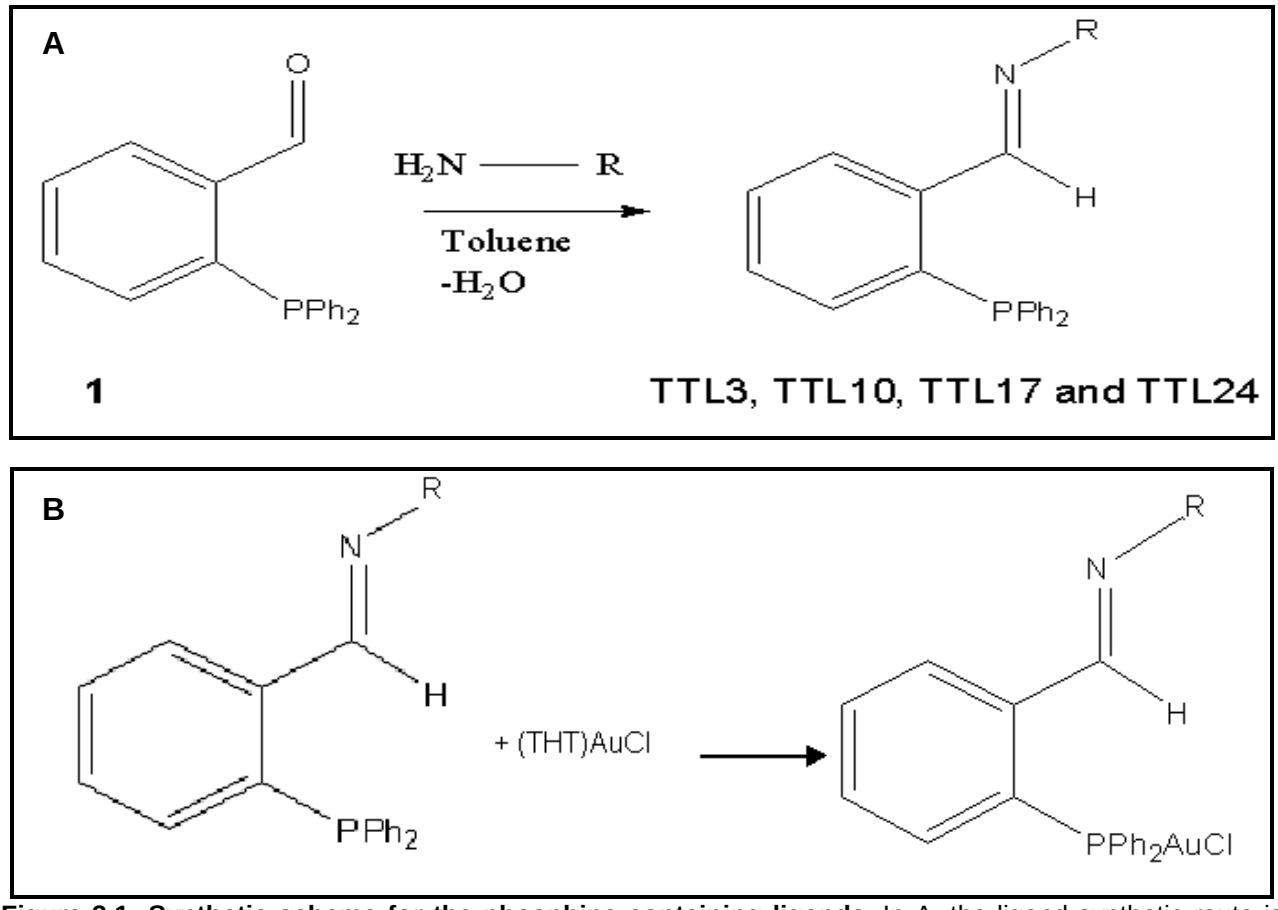

Figure 3.1: Synthetic scheme for the phosphine containing ligands. In A, the ligand synthetic route is shown starting from commercially available 2-(diphenylphosphino)benzaldehyde (**1**). In B, the synthetic route for the corresponding gold(I) complexes using the relevant ligands is shown and involves reactions with (THT)AuCl. R= Phenylethyl (TTL3 and TTL17), R= *N,N*-dimethyl-ethane-1,2-diamine (TTL10, TTL24). These figures were adapted from Traut and Williams (2006).

Table 3.1: The gold(I) phosphine chloride complexes and corresponding ligands (Class I). Ph represents a phenyl ring and the asterisk refers to ligand. The ligands are organic precursors used in the synthesis of the complexes.

Compound structure, code and name	Compound structure, code and name
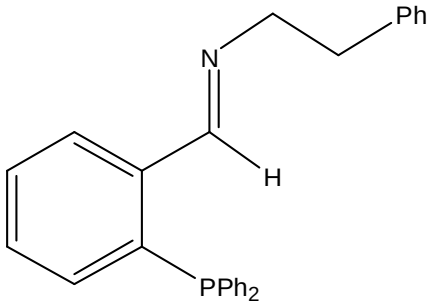 **TTL3*:** (2-diphenylphosphanyl-benzylidene)-phenethyl amine	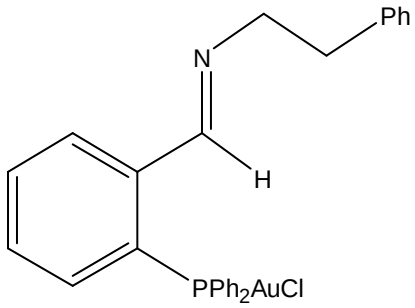 **TTC3:** Benzyl-(2-diphenylphosphanyl-benzylidene)-phenethyl-amine gold(I)chloride
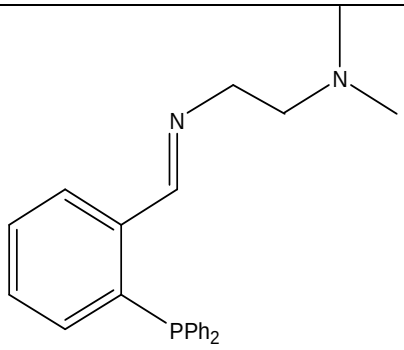 **TTL10*:***N'*-(2-diphenylphosphanyl-benzylidene)-*N,N*-dimethyl-ethane-1,2-diamine	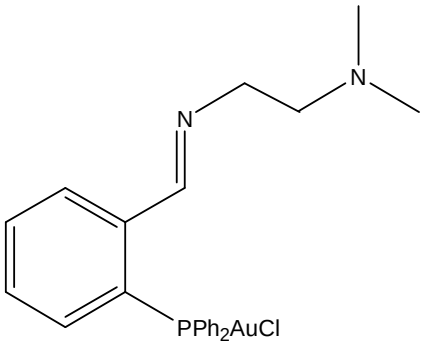 **TTC10**:*N'*-(2-diphenylphosphanyl-benzylidene)-*N,N*-dimethyl-ethane-1,2-diamine gold(I) chloride
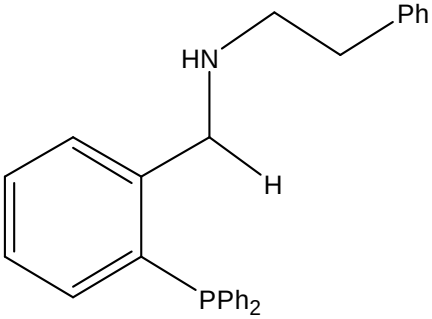 **TTL17:**2-diphenylphosphanyl-benzyl)-phenethyl-amine	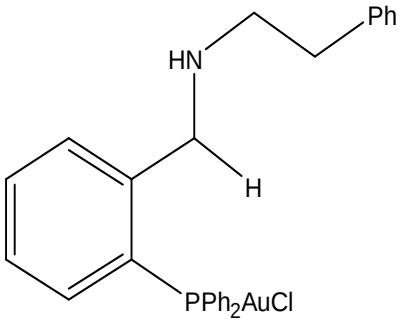 **TTC17:** 2-diphenylphosphanyl-benzyl)-phenethyl-amine gold(I) chloride
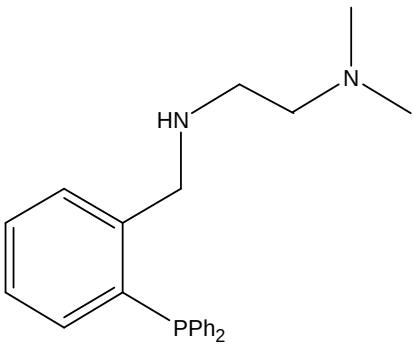 **TTL24:** *N'*-(2-diphenylphosphanyl-benzyl)-*N,N*-dimethyl-ethane-1,2-diamine	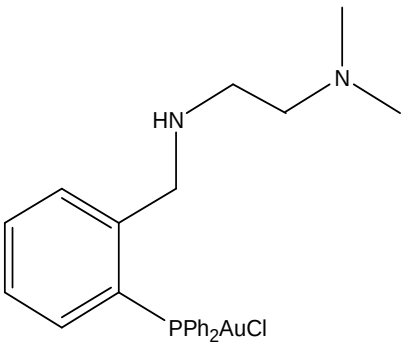 **TTC24:***N'*-(2-diphenylphosphanyl-benzyl)-*N,N*-dimethyl-ethane-1,2-diamine gold(I) chloride

3.2.2 The Bis(phosphino) Hydrazine Gold Chloride-containing Complexes – Class II

The BPH gold(I) chloride group consisted of four gold(I) complexes designated: EK207, EK208, EK219 and EK231. The structure of the hydrazine (backbone structure) for these complexes is shown in Figure 3.2. Synthesis, characterization and analysis for purity were performed by Kriel *et al*., (2007). The authors prepared bisphosphinohydrazine ligand precursors using published methods followed by reaction with either dimethylsulphidegold(I) chloride ($(Me_2S)AuCl$) or (THT)AuCl to produce the corresponding BPH gold(I) complexes (shown in Figure 3.3 A and B and in Table 3.2).

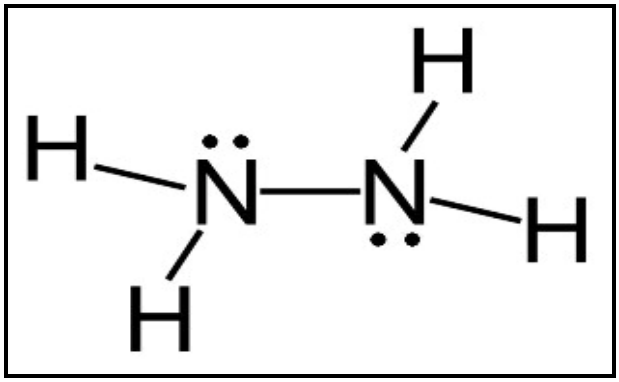

Figure 3.2: The chemical structure of hydrazine (N_2H_4). Hydrazine has two lone pairs of electrons which make it very reactive. The figure was taken from http://toxipedia.org/display/toxipedia/Hydrazine (accessed on the 26/04/2011).

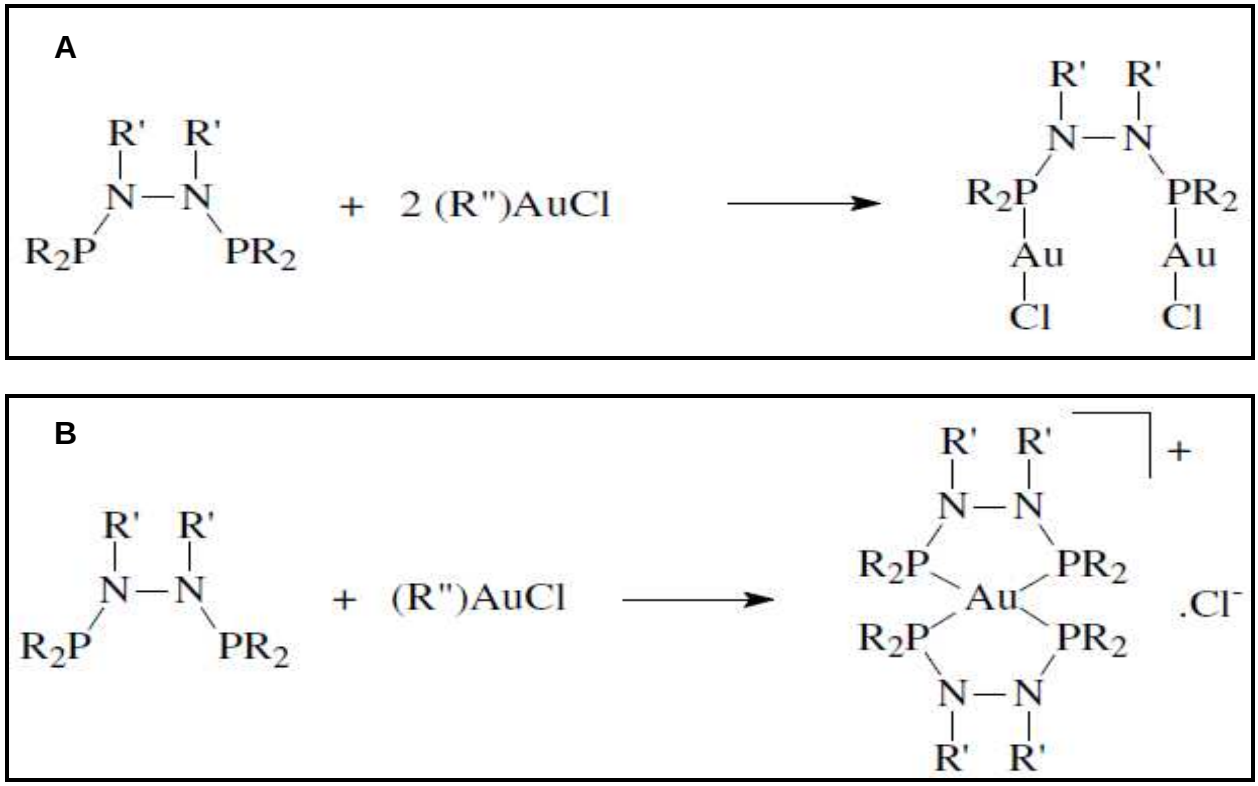

Figure 3.3: Synthetic display for the BPH gold(I) complexes. In (A), R = Ph, R' = Et (EK207), R= PhOMe, R' = Et (EK219), R = Me_2NPh, R' = Et (EK231) and in (B), R= Ph, R' = Et (EK208). In B, R'' = THT or SMe_2 (dimethylsulphide). The figures were taken from Kriel *et al*., (2007).

Table 3.2: BPH gold(I) chloride-containing complexes, Class II. Ph represents a phenyl ring, Et an ethyl group, Me a methyl group and MeO a methoxy.

Compound structure, code and name	Compound structure, code and name
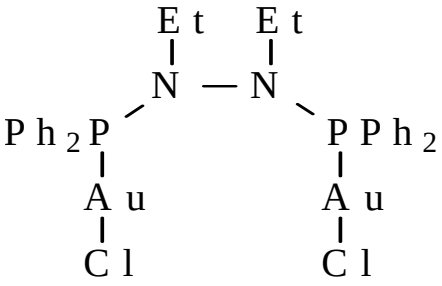 **EK207:**Bis(diphenylphosphino)-1,2-diethylhydrazine di(gold chloride)	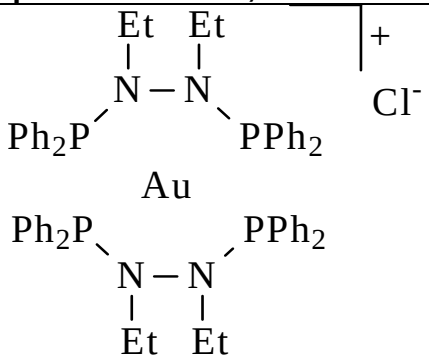 **EK208:** Bis [bis (diphenylphosphino)-1,2-diethylhydrazine] gold chloride
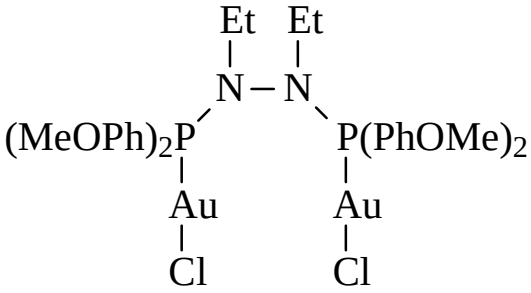 **EK219:** Bis (di (4-methoxyphenyl) phosphine)-1,2-diethylhydrazine di(gold chloride)	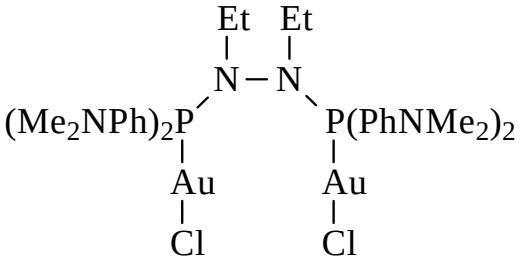 **EK231:** Bis(di(*N,N*-dimethyl aniline)phosphine)-1,2-diethylhydrazine di(gold chloride)

A complex with similar structure to those in this group and to EK208 is the four coordinate gold complex, [1,2-bis(diphenylphosphino)ethane]gold(I) chloride ($Au(DPPE)_2Cl$, please refer to Figure 2.19 for the structure) which was reported in the mid 80s to have promising anti-tumour activity (Fricker, 1996, Berners-Price *et al*., 1986, Mirabelli *et al*., 1986). This complex, in which a phosphine ligand was incorporated, demonstrated activity against leukaemia cells as well as on other tumour models (Berners-Price *et al*., 1986, Mirabelli *et al*., 1986). It was however not entered into clinical trials due to cardiotoxicity problems encountered during pre-clinical toxicology studies (Hoke *et al*., 1989). The toxicity that was observed for this compound was attributable to the high lipophilicity of the phosphine moieties and the ethane backbone which resulted in non specific uptake. The newly synthesized analogues (EK207, EK208, EK219 and EK231) in this study were thus modified through the use of nitrogen heteroatoms to replace the lipophilic ethane bridge present in the parent compound ($Au(DPPE)_2Cl$) by employing a hydrazine bridge instead. It was hoped that the hydrophilic nature of the nitrogen heteroatoms will increase the hydrophilicity of the compounds rendering them more selective and drug-like (Kriel *et al.*, 2007). Although the initial aim of synthesis was to test for anti-cancer activity (explored by Kriel *et al*., 2007), the potential of gold-based compounds as inhibitors of HIV prompted the inclusion of these compounds for testing in this project.

3.2.3 The gold(I) Phosphine Thiolate-based Complexes - Class III

The gold(I) phosphine thiolate group consisted of auranofin designated MCZS2 which is an orally available anti-arthritic agent (Ahmad 2004, Sutton, 1986) that has shown anti-HIV activity *in vivo* (Lewis *et al.,* 2011, Shapiro and Masci, 1996) and two analogues represented by identification codes MCZS1 and MCZS3. The synthesis of MCZS1 and MCZS3 was reported in an AuTEK Biomed communiqué by Sam in 2005. Synthetic intermediates consisting of 2,3,4,6-tetra-O-acetyl-1-thio-B-D-glucopyranose, 1,3,5-triaza-7 phosphaadamantane (PTA), (PTA)AuCl and $[MePTA]^+[CF_3FO_3]^-AuCl$ (where CF_3FO_3 = trifluoromethanesulfonate) were prepared according to literature procedures (see Figure 3.4 for structures). In the case of MCZS1, 2,3,4,6-tetra-O-acetyl-1-thio-B-D-glucopyranose was reacted with (PTA)AuCl while synthesis of MCZS3 involved the reaction of 2,3,4,6-tetra-O-acetyl-1-thio-B-D-glucopyranose with $[MePTA]^+[CF_3FO_3]^-AuCl$. Synthesis was followed by characterisation using ^{31}P NMR. MCZS2 (purchased from Biomol International L.P. (Pennysylvania, USA) was also provided by the AuTEK Biomed group (Mintek, South Africa). The molecular structures, codes and names of the complexes are represented in Table 3.3. This class also included three additional complexes designated PFK174, PFK189 and PFK190 whose structures cannot be disclosed because they are currently part of a patent application for promising anti-cancer activity. The main distinction that the latter has over the former (shown in Table 3.3) is the bimetallic property (containing two gold atoms).

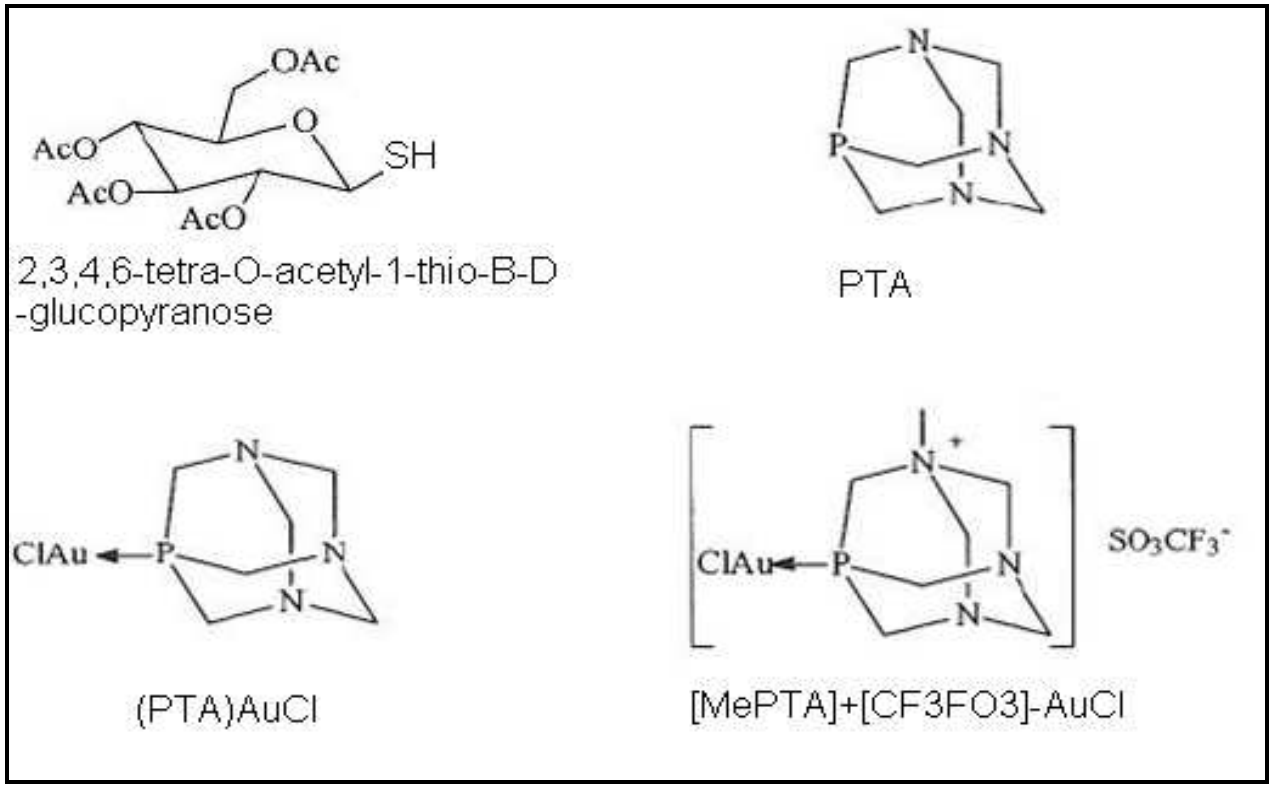

Figure 3.4: The structures of intermediate reagents used for the synthesis of auranofin analogues (MCZS1 and MCZS3). The figure was adapted from Sam, (2005).

Table 3.3: Gold(I) phosphine thiolate complexes. The structures, code names and full chemical names are represented. Ac represent and acetyl group and Et an ethyl group.

Compound structure, code and name	Compound structure, code and name
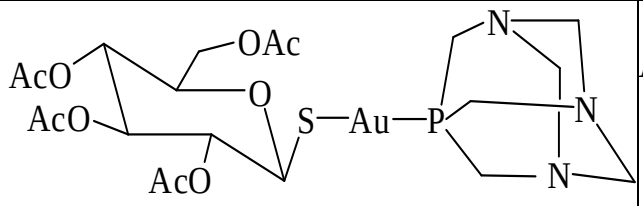 **MCZS1:**(2,3,4,6-tetra-*O*-acetyl-1-thio-*B*-D-glucopyranosato-S-)(1, 3, 5-triaza-7 phosphaadamantane) gold (I)	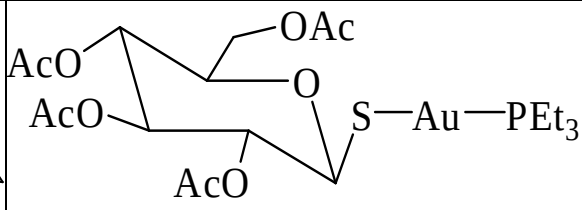 **MCZS2**: (2,3,4,6-tetra-*O*-acetyl-1-thio-*B*-D-glucopyranosato-S-) (triethylphosphine) gold (I)
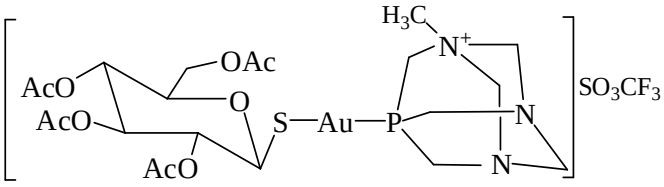 **MCZS3:** (2,3,4,6-tetra-*O*-acetyl-1-thio-*B*-D-glucopyranosato-S-)(1, 3, 5-triaza-7 phosphaadamantane)gold (I) (+1) trifluoromethanesulphonate(-1)	

3.2.4 The gold(III) Tscs-based Complexes – Class IV

The Tscs compounds included ligands PFK5, PFK6, PFK38 and PFK39 and their corresponding complexes designated PFK7, PFK8, PFK43 and PFK41 respectively. The synthesis and anti-HIV activity has been compiled in a manuscript that has been accepted for publication by the Journal of Inorganic Biochemistry (Fonteh *et al*., 2011). The gold starting material, $HAuCl_4.4H_2O$, was synthesised using procedures reported by Block (1953) while the bis(Tscs) ligands (PFK5, PFK6, PFK38 and PFK39) were synthesised according to methods by West *et al*., 1997. This was followed by the complexation reaction which led to the production of PFK7, PFK8, PFK43 and PFK43 (the synthetic route is shown in Figure 3.5). Synthesis was followed by characterisation using ^{1}H NMR, infrared spectroscopy and microanalysis (Fonteh *et al*., 2011). The structures of the ligands and complexes are shown in Table 3.4. These compounds unlike the first two classes (phosphine and the BPH containing compounds) and MCZS1, MCZS2 and MCZS3 were newly synthesised and tested for the first time in this study for anti-HIV activity. The complexes also differ from the first three classes in the oxidation state which is +3 unlike +1. Although Bottenus *et al*., (2010) recently reported the synthesis of complex PFK8, the synthetic protocol used is different from that described by Fonteh *et al.*, (2011).

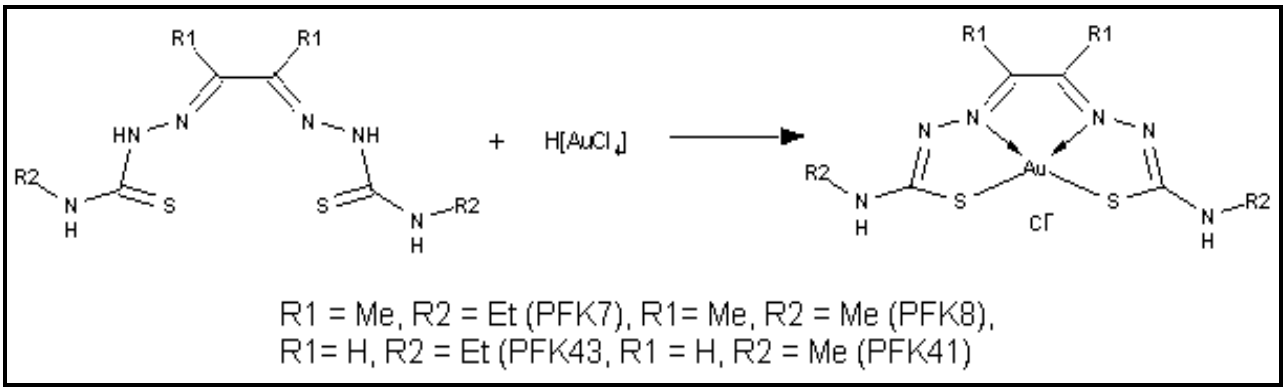

Figure 3.5: Synthetic scheme for the bisthisemicabarzonate complexes (PFK7, PFK8, PFK43 and PFK41). The complexes were synthesised from the respective ligands (PFK5, PFK6, PFK38 and PFK39). This figure was taken from Fonteh *et al.,* (2011).

Table 3.4: The gold(III) thiosemicarbazonate complexes and corresponding precursors. The asterisk represents ligands. (Fonteh *et al*., 2011).

Compound structure, code and name	Compound structure, code and name
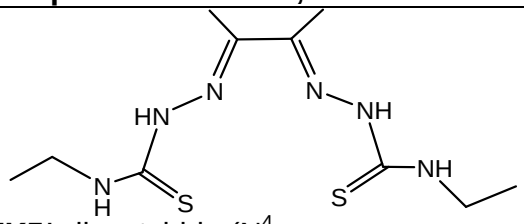 **PFK5*:**diacetyl-bis-(N^4-ethylthiosemicarbazone)	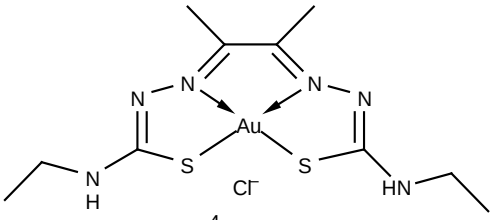 **PFK7:**diacetyl-bis-(N^4-ethylthiosemicarbazonate)gold(III)chloride
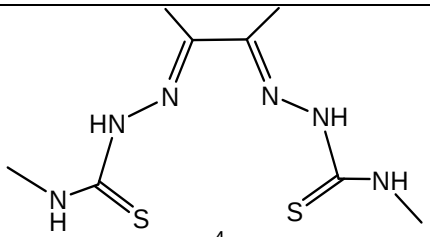 **PFK6*:**diacetyl-bis-(N^4-methylthiosemicarbazone)	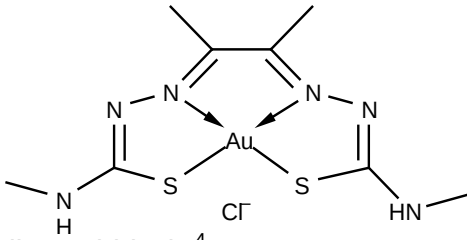 **PFK8:**diacetyl-bis-(N^4-methylthiosemicarbazonate)gold(III)chloride
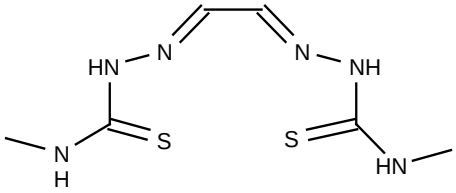 **PFK38*:**diglyoxal-bis-(N^4-methylthiosemicarbazone)	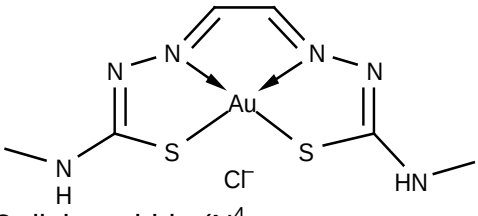 **PFK43:**diglyoxal-bis-(N^4-methylthiosemicarbazonate)gold(III)chloride
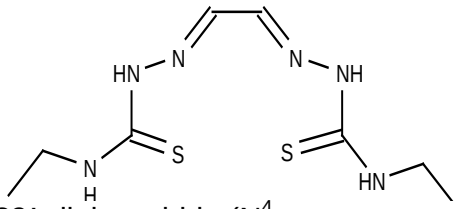 **PFK39*:**diglyoxal-bis-(N^4-ethylthiosemicarbazone)	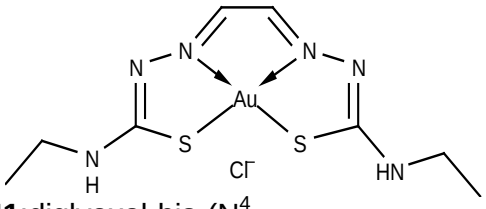 **PFK41**:diglyoxal-bis-(N^4-ethylthiosemicarbazonate)gold(III)chloride

3.2.5 The Gold(III) Pyrazolyl-based Complex – Class V

The last class (V) consisting of only one member is the gold(III) pyrazolyl-based complex designated KFK154b. The synthesis, purity and characterization, activity on HIV RT and PR was reported by Fonteh *et al*., (2009). Synthesis involved reacting $H[AuCl_4]$ with bis(3,5-dimethylpyrazolyl)acetic acid as shown in the synthetic reaction in Figure 3.6. The structure of the complex is shown in Table 3.5.

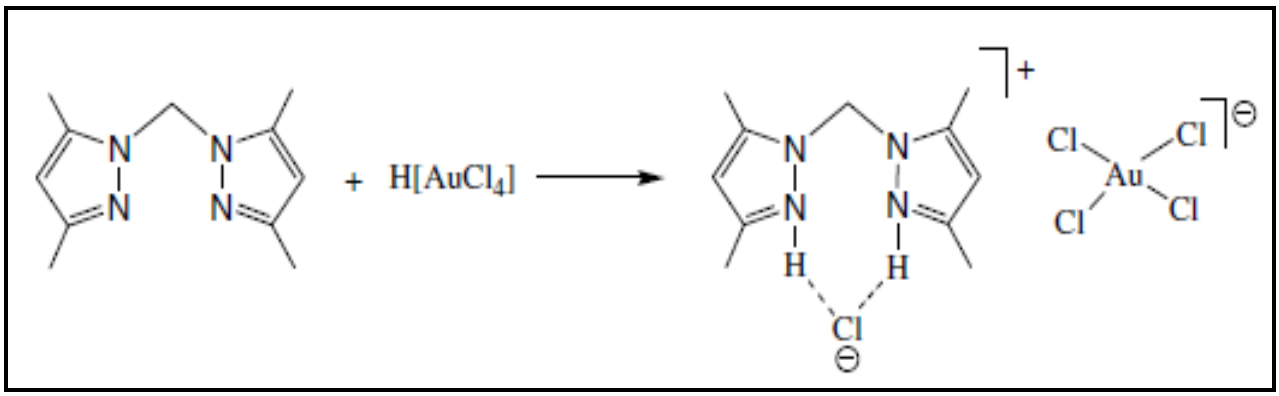

Figure 3.6: Synthetic scheme for tetra-chloro-(bis-(3,5-dimethylpyrazolyl)methane)gold (III)chloride. The Figure was taken from Fonteh *et al*., (2009).

Table 3.5: The pyrazolyl gold(III) complex, (Fonteh *et al*., 2009).

Compound structure, code and name
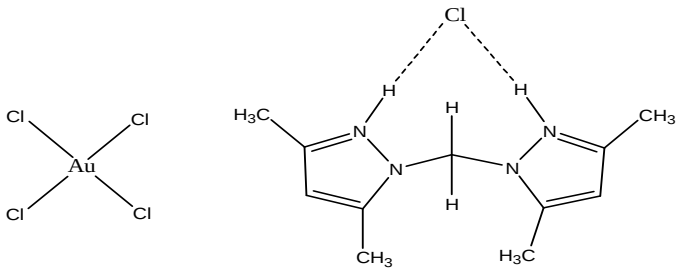
KFK154b: Tetra-chloro-(bis-(3,5-dimethylpyrazolyl)methane)gold (III)chloride

In Table 3.6 important additional information on the compounds is provided and includes relative Mr, the number of rotatable bonds and the number of hydrogen bond (H-bond) donors (counted as number of hydrogens attached to N or O) and acceptors (approximated as the number of N or O atoms). Some of these parameters were incorporated by Lipinski *et al*., in 1997 in coining the rule of 5 regarding absorption (one of the drug-like parameters). The number of rotatable bonds is related to molecular flexibility and gives an idea of the number of conformations that can be generated (Höltje *et al*, 2003) to allow it to interact with an active site in receptor/ligand interactions (covered in chapter 5). For ease of reference, the compounds tested in the proof of concept study (mentioned in chapter 2 section 2.5) will sometimes be referred to as “compounds tested in prior study” from here onwards. These are the first fifteen and last compound in Table 3.6. Tables 3.1 to 3.6 will be referenced throughout this report to refer to the different compounds in the different classes.

Table 3.6: Additional compound structural information. Molecular formula, Mr, the number of rotatable bonds, H-bond donors and acceptors are shown. The ligands are shaded in gray. The various classes of the compounds are also represented.

Class	Compound code	Molecular formula	Mr (g/mol)	Rotatable bonds	H-bond donors	H-bond acceptors
I	TTL3	C27 H24 N P	393.17	7	0	2
	TTC3	C27 H24 Au Cl N P	625.10	8	0	1
	TTL10	C23 H25 N2 P	360.18	7	0	3
	TTC10	C23 H25 Au Cl N2 P	592.11	8	0	2
	TTL17	C27 H26 N P	395.18	8	1	2
	TTC17	C27 H26 Au Cl N P	627.12	9	1	1
	TTL24	C23 H27 N2 P	362.19	8	1	3
	TTC24	C23 H27 Au Cl N2 P	594.13	9	1	2
II	EK207	C28 H30 Au2 Cl2 N2 P2	920.06	11	0	2
	EK208	C56 H64 Au Cl N4 P4	1148.34	18	4	4
	EK219	C32 H38 Au2 Cl2 N2 O4 P2	1040.10	15	0	6
	EK231	C36 H50 Au2 Cl2 N6 P2	1092.23	15	0	6
III	MCZS1	C20 H31 Au N3 O9 P S	717.12	11	0	13
	MCZS2	C20 H34 Au O9 P S	678.13	14	0	10
	MCZS3	C22 H34 Au F3 N3 O12 P S2	881.09	13	0	15
IV	PFK5	C10 H20 N6 S2	288.12	9	4	4
	PFK7	C10 H18 Au Cl N6 S2	518.04	4	2	4
	PFK6	C8 H16 N6 S2	260.09	7	4	4
	PFK8	C8 H14 Au Cl N6 S2	490.01	2	2	4
	PFK38	C8 H16 N6 S2	232.06	7	4	4
	PFK43	C8 H14 Au Cl N6 S2	461.98	2	2	4
	PFK39	C6 H12 N6 S2	260.09	9	4	4
	PFK41	C6 H10 Au Cl N6 S2	490.01	4	2	4
V	KFK154b	C11H20AuCl5N4	582.5	2	2	1

In addition to screening the gold-based complexes, four platinum-based complexes of the Tscs ligands (PFK5, 6, 38 and 39, Table 3.4) were also assayed for HIV inhibitory effects. The platinum-based complexes had no inhibitory effect on the activity of HIV RT and PR both *in vitro* and *in silico*. A manuscript describing synthesis of these Pt-based compounds and possible reasons for the lack of activity on RT and PR enzymes is in preparation (by Keter *et al*.,).

3.3 MATERIALS AND METHODS

In the materials and methods section of this chapter and in chapter 4 and 5, the principles or background of the techniques employed will also be provided.

3.3.1 NMR Studies for Stability Determination

Compounds for HTS are normally dissolved in DMSO. The hygroscopic nature of DMSO could unfortunately lead to stability issues. To investigate the structural stability of the complexes, NMR spectra of the complexes dissolved in DMSO was obtained on immediate dissolution and later at 24 h and after one week at two relevant temperatures (storage and

physiological). The fact that many nuclei have magnetic properties that arise from the spin of subatomic particles (protons and neutrons) in their nucleus makes it possible to observe their spectra which results from the overall spin. In some nuclei such as ^{12}C, ^{16}O and ^{32}S, the overall spin cancels out while in others such as ^{1}H, ^{13}C, ^{19}F and ^{31}P, it does not, such that an overall spin and therefore spectra are produced. Gold unfortunately does not have a useful NMR nucleus (Shaw III, 1999). NMR characterisation of gold complexes therefore makes use of the presence of other magnetic nuclei such as ^{1}H and ^{31}P.

A minimum of 10 mg/mL of representative gold complexes (TTC3, EK231, MCZS3, PFK7, PFK174 and KFK154) from each class was subjected to ^{1}H and or ^{31}P NMR spectra analysis (300 MHz Anova Varian spectrometer, Varian Inc., Oxford, England) following dissolution in *d6*-DMSO (newly opened to minimise the presence of water). The spectra obtained were labelled day zero spectra. Day zero samples and a duplicate were then stored at -20 and 37 ºC respectively and analysed again after 24 h and on day 7 to determine compound stability over this time period compared to day zero. ^{1}H chemical shifts of the complexes were referenced to the signals of the residual proton peak of the NMR solvent while those of ^{31}P were referenced to a phosphorous standard (85% H_3PO_4) and quoted in parts per million (ppm).

Due to concerns that compound stability and precipitation from solution could be significantly enhanced over longer periods of storage in DMSO, dissolved compounds were generally not stored for longer than one week before use in bioassays. It has been shown that compounds dissolved in DMSO are capable of precipitating out of solution by the third week (Waybright *et al*., 2009). Since the compounds were not used beyond a week after dissolution in DMSO, NMR spectroscopy studies were therefore limited to one week. Another precautionary measure to sustain stability was the fact that the compounds were maintained in desiccated forms at -20 ºC and only working stocks sufficient for use within a week were prepared.

3.3.2 *In Silico* ADMET Predictions

In order to perform the ADMET predictions, 2D sketches of the compounds were drawn in ChemDraw (CambridgeSoft, PerkinElmer Inc., USA) and saved as structural data files (sdf) or molecular (mol) file formats which are formats compatible with the Discovery Studio® (Accelrys®, California, USA) computational software package that was used for the predictions. Prior to initiating the runs, a compound preparative phase was performed. This involved checking and correcting valencies, adding hydrogens, applying force fields and geometry optimisation through energy minimization. The energy minimisation was performed using a CHARMm (Chemistry at Harvard Macromolecular mechanics) force field which updates the coordinates of the molecule (based on reference values, Höltje *et al*. 2003) and adds energy properties. By using these computations, the structures were given more relaxed

and better geometries with energy minima. The computational predictions were performed on an LG Intel® Core™ 2 Duo CPU 2.2 GHz processor, 1.97 GB RAM with Windows XP professional version 2002 operating system which are the minimum system requirements recommended by DS® for such studies.

The ADMET protocol in DS® which aids in the prediction of aqueous solubility, BBB penetration, CYP inhibition, hepatotoxicity, HIA and PPB of the compounds was used for predicting drug-likeness. This protocol includes the models by Egan *et al*., (2000) and Egan and Lauri, (2002) for HIA which incorporates AlogP98 (atom-based log P or lipophilicity) and polar surface area (PSA, related to the H-bonding ability). Also included are the models of Cheng and Merz, (2003) for aqueous solubility, Egan and Lauri, (2002) for BBB penetration, Susnow and Dixon, (2003) for CYP inhibition, Cheng and Dixon, (2003) for hepatotoxicity and Dixon and Merz, (2001) for PPB predictions. These models come with rankings for each ADMET descriptor that helps in predicting the confidence of the estimations. The various models were derived from diverse datasets of compounds with a wide range of chemical families from both the literature and those in clinical use, representative of each descriptor and subsequently validated using training sets.

Lipophilicity (presented as AlogP98 in the *in silico* studies and as Log P in the shake flask assay in sections 3.3.3) is applicable to all the ADMET parameters and is not a standalone property. Lipophilicity is used to assess biological parameters relevant to drug action such as lipid solubility, tissue distribution, receptor binding, cellular uptake, metabolism and bioavailability (Ghose *et al*., 1998) which are all related to the ADMET descriptors. It is the driving force around transmembrane transport and additionally helps to determine pharmacological activity and toxicity (Gombar and Enslein, 1996). The importance of lipophilicity as a physicochemical property in drug design means it plays a major role in determining drug-likeness of potential compounds.

3.3.2.1 Human intestinal absorption prediction model

The HIA model was developed using 182 compounds in the dataset with descriptors that include AlogP98 and PSA (Egan *et al*., 2000, Egan and Lauri, 2002). The model includes a 95% confidence ellipse and a robust 99% confidence ellipse in the ADMET PSA and AlogP98 plane. These ellipses define regions where well-absorbed (>90% absorbed) and poorly absorbed (<30% absorbed) compounds are expected to be found. Four prediction levels are provided to aid in the classification: 0 = good, 1 = moderate, 2 = poor and 3 = very poor absorption.

3.3.2.2 Aqueous solubility prediction model

A predictive model for aqueous solubility was determined by Cheng and Merz (2003) using a data set of 775 compounds with Mr between 70 and 800 g/moL. A validation set of

1665 compounds from Physician's desk References and Comprehensive Medicinal Chemistry databases were used and the findings from the predictions agreed with experimental values. Six solubility levels are described, 0 = extremely low (log(Sw)< -0.8, 1 = very low but possible (-0.8< log (Sw)< -6.0), 2 = low (-6.0<log(Sw) < -4.0), 3 = good (-4<log (Sw) < -2.0), 4 = optimal (-2.0<log(Sw) = 0.0), 5 = too soluble (0.0 <log(Sw) and 6 = warning; molecules with one or more unknown AlogP98 type are present, where log Sw = solubility in water at 25 ºC and pH 7.0.

3.3.2.3 Blood brain barrier penetration prediction model

The BBB penetration prediction also developed by Egan and Lauri (2002) incorporates the AlogP98 as well as PSA plane. Confidence ellipses were also used in the prediction and included a 95 and 99% ellipse. Although the data is interpreted similarly to those of the HIA ellipses, the planes are different from those used in the HIA model. The model was derived from over 800 compounds that are known to enter the central nervous system after oral administration. Four prediction levels within the ellipses were determined for this model and include: 0 = very high penetrant (logBB≥0.7), 1 = high (0≤logBB<0.7), 2 = medium (0.52<logBB<0), 3 = low (logBB≤-0.52), 4 = undefined, where logBB = logarithm of blood brain penetration.

3.3.2.4 Cytochrome P4502D6 prediction model

The model derived by Susnow and Dixon (2003) for predicting CYP inhibition was obtained from a diverse data set of 100 compounds using 2D chemical structures as input. The model classifies compounds as either 0 (non inhibitor, i.e. unlikely to inhibit the CYP2D6 enzyme with probability <0.5) or 1(inhibitor, likely to inhibit CYP2D6 enzyme with probability >0.05) and provides an average value of confidence.

3.3.2.5 Hepatotoxicity prediction model

Drug induced liver injury is responsible for 5% of all hospital admissions and 50% of all acute liver failures (Ostapowicz *et al*., 2002) making the identification of potential hepatotoxic compounds crucial during drug development. The training set of compounds that were employed by Cheng and Dixon (2003) for hepatotoxicity prediction was from a diverse set of compounds causing all types of liver injuries and spanning a wide range of chemical families. The resulting training set of compounds included 382 drug and drug-like compounds of various therapeutic classes known to exhibit liver toxicity. Using only 2D information of the compounds provided, the model predicts with > 80% accuracy, the potential for the occurrence of dose-dependent human hepatotoxicity of any compound. The model classifies compounds as either "toxic" (1) or "nontoxic" (0) and provides a confidence level indicator of the likelihood of the model's predictive accuracy.

3.3.2.6 Plasma protein binding prediction model

The ADMET PPB model derived by Dixon and Merz (2001) predicts the likelihood of a compound binding to carrier proteins in blood. The properties computed in this model include the AlogP98, unknown AlogP98 and the PPB levels. The classification levels include 0 = likelihood of a compound binding by <90%, 1 = likelihood of binding by > 90% and 2 = likelihood of binding by > 95%. These levels are scored based on the flagging of marker molecules in the compound.

3.3.2.7Currently available ARV drugs as Controls for ADMET predictions

Currently available ARV drugs were used as controls for supporting the predictions as well as for providing data that could allow for commentary on the drug-like properties of the compounds studied here with respect to these available drugs. Molecular structures of the controls in the sdf format were obtained from the protein data bank (PDB, at http://www.ncbi.nlm.nih.gov/pccompound).

3.3.3 Shake Flask Method for Lipophilicity Measurement

In addition to using DS® to computationally determine the lipophilicity of the compounds, an experimental shake flask method was also used. This was employed to complement or confirm the theoretical predictions. The shake flask method is a traditional method for determining lipophilicity and involves the introduction of the test compound to two phases (n-octanol and water) into a separating funnel (Danielsson and Zhang, 1996). The funnel is then shaken for a period long enough for equilibrium to be achieved. The concentration of the compound of interest in each phase is determined after phase separation by measuring absorbance.

The confirmation assay was performed for two complexes only, PFK7 and PFK8 which were found to be soluble in both the octanol and water phases used for determining partition coefficient or lipophilicity. Solubility in both phases obviates one of the shortcomings of the shake flask method. This is because lipophilicity values are difficult to obtain for compounds which are very lipophilic or very hydrophilic since a proper ratio or partition coefficient between the two phases cannot be obtained.

The assay was performed using a modified shake flask method (Yousif *et al*., 2009). Phosphate buffered saline (PBS, sterile filtered, pH 7.4) was used as the aqueous phase because it is more physiologically relevant while the organic (or lipid phase) was 1-octanol (Sigma Aldrich, Missouri USA, ≥ 99%). The physicochemical similarity of 1-octanol to lipids makes it a natural choice as a hydrophobic solvent (Ghose *et al*., 1998). The complexes were dissolved in DMSO and diluted with PBS to a final concentration of 200 µM. An equal volume of 1-octanol was added to the solution and both fractions were subjected to shaking (45 rpm, 30 min) on an Intelli Mixer (Sky Line, Riga, Latvia). Once equilibrium had been attained, the

two phases (organic and aqueous phases) were separated after allowing the mixture to stand for 5 min. Serial 2 fold dilutions (200 to 0.625 µM) for each compound in both the 1-octanol and PBS phases were used as standards in determining the concentration of those of the test samples. Both the standards and different phases of each of the compounds were loaded onto 96 well plates (tissue culture grade, Nunc^{TM}, Roskilde, Denmark) and the absorbance obtained by UV-Vis spectroscopy at 375 nm using a Multiskan Ascent® spectrophotometer (Labsystems, Helsinki, Finland). Plots of the standard curves were used in obtaining the concentrations of the samples. Log P was defined and calculated as the logarithm of the ratio of the concentrations of the compound in the organic and aqueous phases (Log P=Log {[compound$_{(org)}$]/[compound$_{(aq)}$]} where org = organic phase and aq = aqueous phase.

3.4 RESULTS AND DISCUSSION

3.4.1 NMR Profiles

The NMR profiles of the complexes were obtained on day zero to serve as reference spectra and for comparison with those obtained at synthesis. Subsequently two more spectra were obtained at 24 h and after 7 days (stored at -20 and 37 ºC) to determine stability w.r.t. the day zero sample. Because the characterisation of the structures had been performed and confirmed by the chemists, emphasis was placed on identifying any differences and changes in the spectra over time at these temperatures. When using NMR for stability analysis one expects spectra taken at different time points to exhibit peaks at the same chemical shifts irrespective of when they were collected. If there is a change in the observed shifts or appearance of new signals over time, this can be interpreted as possible degradation or the formation of new products. It should however be kept in mind that some structural changes which could have occurred over time may not be detectable by NMR either as a result of spectral overlap (resulting from similarity in backbone structures of breakdown products) or as a result of low sensitivity (Kenseth and Coldiron, 2004). In the next subsections, the outcomes from the NMR analysis for the different complexes that were analysed will be provided. The actual spectra are provided in the appendix for those complexes for which chemical shifts were observed.

3.4.1.1 ^{31}P and ^{1}H NMR chemical shifts of the gold(I) phosphine chloride complex TTC3

The ^{31}P NMR of TTC3 remained unchanged over 7 days at -20 and 37 ºC with a consistent peak at 33.9 ppm. In the chemical shifts in the ^{1}H NMR were maintained except for the presence of a water signal at 3.3 ppm (Gottlieb *et al*., 1997) which was present on day zero, becoming more prominent after 24 h and 7 days later and affecting resolution (Figure A3.1). The spectrum on day zero for this complex suggests that water was present in the compound even as a powder (Figure A3.1A). This means that the compound was hygroscopic (taking up some water from the atmosphere in the course of storage) which was further

compounded by DMSO's hygroscopic nature, evident from the more prominent water peak after 24 h and 7 days (Figure A3.1B and C). The increase in the water peak must have been enhanced by the fact that the same sample was intermittently opened and closed during the analysis times (24 h and 7 days later). The hygroscopic limitation associated with DMSO emphasises the importance of storing DMSO stocks and DMSO dissolved compounds in single use vials or under inert gas. By so doing, complications (e.g. compound precipitating out of solution) that can arise from having water in a DMSO solution of potential bioactive compounds can be avoided or reduced (unless in a case where the compound itself is hygroscopic).

3.4.1.2 ^{31}P and ^{1}H NMR chemical shifts of the BPH gold(I) chloride complex EK231

The ^{31}P NMR spectra for EK231 over 7 days and at the two different temperatures also remained unchanged with a consistent peak at 83.9 ppm. As was the case for TTC3, the water peak in the ^{1}H NMR (absent on day zero) was prominent after 24 h and at 7 days, increasing in area and height over this time. The rest of the shifts remained stable throughout the analysis except for a new peak at 2.4 ppm (after 24 h and on the 7th day) suggestive of the presence of acetone which was used in cleaning the NMR tubes.

The stability of this complex and that of TTC3 (seen in the ^{31}P NMR) is thought to be related to the stability conferred by the covalent bond between P of the phosphine ligand and gold (Parish and Cottrill, 1987).

3.4.1.3 ^{31}P and ^{1}H NMR chemical shifts of the gold(I) thiolate complexes MCZS3 and PFK174

The ^{31}P NMR peak for MCZS3 on day zero was absent possibly because of poor solubility (Figure A3.2A). This compound which was provided as a powder was noted to be hygroscopic absorbing water from the atmosphere. The poor solubility in DMSO may be as a result of precipitation of the compound out of solution due to the presence of water. In the ^{1}H NMR spectrum, the broad peak at 3.4 ppm is likely HDO (semi heavy water) resulting from *d6*-DMSO exchanging a deuterium atom with hydrogen atom of water (deuterium exchange). According to the spectrum, the backbone phosphine and acetylated sugar moieties are intact but impurities (including HDO and possibly H_2O) are evident (Figure A3.2B). Subsequent analysis after 24 h and 7 days was not done due to the evident poor solubility observed as precipitation which ended up limiting sample concentration for ^{31}P NMR analysis. In addition, since this compound did not show promising activity during inhibition studies (reported in chapter 4 and 5), the need to pursue stability and storage properties was considered not important for this study.

A ^{31}P NMR peak for PFK174 was also evidently absent and the reason for this was also ascribed to poor solubility. In the ^{1}H NMR spectra, a water peak was evident on day zero (inherent hygroscopic ability) but most of the ^{1}H shifts were poorly resolved. Similar to MCZS3,

the poorly resolved peaks probably arose from the poor solubility that was observed for this compound. At the minimum required concentration (10 mg/mL) for NMR analysis, the complex was visibly precipitating out of *d6*-DMSO. The fact that solubility (both in DMSO and in aqueous media) can affect bioassay reproducibility means that for this compound to be successfully used as a drug, it would require some form of modification to enhance solubility. Fortunately, it may not be necessary to do this for PFK174 and its analogues because outstanding inhibitory effects were not observed in the inhibition studies (discussed in chapters 4 and 5). This compound which is one of the bimetallic compounds in class III may however need further attention in determining its solubility especially for the anti-cancer project for which a patent application has been launched for the outstanding anti-cancer activity.

In the ^{1}H NMR spectrum the presence of a water peak at 3.3 ppm was also evident (day zero), subsequently becoming more prominent. This finding was similar to that observed the ^{1}H spectra of TTC3 and EK231 and was thought to be as a result of DMSO's hygroscopic nature after intermittent opening at the 24th hour and latter at 7 days.

The limited solubility observed for complexes MCZS3 and PFK174 in *d6*-DMSO and the observed absence of a ^{31}P peak may be related to the fact that these complexes contained water which is known to facilitate the precipitation of compounds out of DMSO solution (Ellson *et al*., 2005). Alternatively, the presence of water in these complexes (which was more prominent than for the others) might have suppressed the ^{1}P NMR peaks to undetectable levels.

3.4.1.4 ^{1}H NMR chemical shifts of the gold(III) thiosemicarbazonate complex, PFK7

Only the ^{1}H NMR spectrum of PFK7 was obtained since the compound does not contain phosphorous as one of its atoms. With respect to the ^{1}H spectrum, the chemical shifts for this complex appeared stable over time except for the presence of the water peak at 3.3 ppm (Gottlieb *et al*., 1997) on day zero which became more prominent at 24 h and 7 days at 37 ºC (shown in Figure A3.3). The increase in the water peak after 24 h and 7 days was also attributed to DMSO's hygroscopic nature.

3.4.1.5 ^{1}H NMR chemical shifts of the gold(III) pyrazolyl complex, KFK154b

Only the ^{1}H NMR spectrum for this compound was obtained as well since there is no phosphorous environment. The water peak at 3.33 ppm seen on day zero for the other complexes and at 24 h and 7 days later at both -20 and 37 ºC was absent for this complex. The only new peak that was observed appeared around 4.7 ppm after 24 h (Figure A3.4B) and was present on analysis on day 7 (Figure A3.4C). The peak at 4.7 ppm indicated the presence of impurities such as deuterated water (D_2O, Gottlieb *et al.*, 1997). It is not clear why the water peak at 3.33 ppm was absent at 24 h and after 7 days since all the samples were handled the same. The deuterated water peak at 4.7 ppm may have compensated for this or alternatively,

this compound did not have a hygroscopic tendency like the others did. According to the ^{1}H NMR of the compound, the backbone structure remained intact over the analysis time.

3.4.1.6 Summary of NMR Stability Profiles

Table 3.7 is a summary of the NMR profile changes that were observed. A water peak in the ^{1}H NMR spectrum (at 3.33 ppm, Gottlieb *et al*., 1997) of complexes TTC3, EK231, MCZS3, PFK174 and PFK7 was the most visible change that was seen over time. A water peak was evident in the spectra of complexes TTC3, MCZS3, PFK174 and PFK7 (suggesting that these complexes had hygroscopic tendencies) on day zero and became prominent by 24 h and 7 days later. In the spectra of EK231, a water peak was visible at 24 h and at 7 days but not on day zero. The presence of water in DMSO solutions of compounds causes precipitation of dissolved compounds and can lead to concentrations disparities in *in vitro* tests. According to Ellson *et al*., (2005), only minimal degradation can result probably explaining why all the compounds tested above remained relatively intact (as seen from the uniformity in ^{1}H and ^{31}P environments and the overall backbone structures) even in the presence of water. To minimise DMSOs' effects in our samples, compounds were aliquoted and stored in single use vials. Compounds dissolved and stored at -20 ºC for subsequent assays were also stored in single use volumes.

With regards to compound stability, the backbone structures of the compounds appeared to be maintained suggesting stability. The only new peaks were the water peak found in the spectra of complexes TTC3, MCZS3, PFK174 and PFK7 on day zero which became prominent at 24 h and 7 days. In the ^{1}H spectra of EK231 acetone was present as an impurity while a new peak in the spectrum of KFK154b at 4.7 ppm after 24 h and on day 7 following storage at -20 ºC and at 37 ºC (Figure A3.4B) was suggestive of the presence of deuterated water (Gottlieb *et al*., 1997). Poor solubility of PFK174 led to poorly resolved ^{1}H NMR and no ^{31}P shifts. It is possible that structural changes can appear especially at higher temperatures after longer time periods (has been seen for compounds stored at 4 ºC dissolved in DMSO). However, ^{31}P NMR shifts of some of these complexes after 4 months in DMSO at -20 ºC, (Fonteh and Meyer, 2008) maintained chemical shifts. The fact that the compounds in this study were never used for bioassays beyond one week (dissolved in DMSO), meant stability studies after one week were not necessary. Although the backbone structures of the compounds appeared to be maintained, compounds with inherent hygroscopic abilities e.g. TTC3, MCZS3, PFK174 and PFK7 can lead to varying data in bioassays resulting from precipitation in DMSO.

Table 3.7: Stability profile summary. ^{1}H and ^{31}P NMR spectra of the complexes were acquired on immediate dissolution in *d6*-DMSO, at 24 h, and 7 days later (stored at -20 and 37 ºC). N/A is not applicable

Complex	^{1}H NMR profile changes		^{31}P profile changes over time	Conclusion (overall backbone structure)
	Day zero	over time (24 h and 7 days)		
TTC3	H_2O peak	Increasing	Stable	Intact but compound may be hygroscopic
EK231		H_2O peak and acetone	Stable	No water peak on day zero but present after 24h
MCZS3	HDO and H_2O	Not done	Nil (limited solubility)	Intact but contains impurities and is hygroscopic
PFK174	H_2O peak	Increasing	Nil (limited solubility)	Poorly resolved ^{1}H spectra. Compound may be hygroscopic
PFK7	H_2O peak	Increasing	N/A	Intact but compound may be hygroscopic.
KFK154b		New peak at 4.6ppm	N/A	Backbone intact with impurity at 4.6 ppm suggestive of D_2O.

3.4.2 *In silico* ADMET Predictions

Drug-likeness predictions for the compounds using the ADMET protocol in DS® are shown in Table 3.8A. Predictions for existing ARV drugs are shown in Table 3.8B and were included for comparison purposes with those of the compounds studied here. Auranofin/MCZS2 (a gold-based drug) was also used as reference since the literature contains information on its drug-likeness.

3.4.2.1 Prediction of human intestinal absorption

HIA was predicted to be good (0) to moderate (1) for sixteen of the compounds namely four of the phosphine compounds (TTL10, TTC10 and TTL24, TTC24), three of the gold(I) phosphine thiolate complexes (MCZS1, MCZS2 and MCZS3), the Tscs ligands and complementary gold(III) complexes (PFK5, PFK6, PFK38, PFK39 and PFK7, PFK8, PFK41, PFK43 respectively) and the gold(III) pyrazolyl complex KFK154B (Table 3.8A). Very low (3) HIA levels were predicted for three phosphine chloride compounds (TTL3, TTC3, and TTL17), the BPH gold(I) complexes (EK207, EK208, EK219 and EK231) and the bimetallic complexes; PFK174, PFK189 and PFK190 of class III (Table 3.8A). TTC17 was the only complex ranked to be low (2) in absorption. The compounds predicted to have poor HIA also meet some of the criteria of “Lipinski’s rule of five” which states that poor absorption or permeation is more likely when there are > 5 H-bond donors, >10 H-bond acceptors, the Mr is > 500 and the calculated log P is > 5 (Lipinski *et al*., 1997). The BPH complexes (EK207, EK208, EK219, EK231) and the gold(I) thiolate complexes (PFK174, PFK189 and PFK190) as well as TTC3 with very low solubility predictions have molecular weights of >500 (Table 3.6) as well as lipophilicity values of >5 (Table 3.8A). TTL3 and TTL17 (phosphine compounds), predicted to have very low HIA (Table 3.8A), also met one of “Lipinski’s rule of five” by having lipophilicity predictions of >5.

Table 3.8A: ADMET prediction scores for the compounds. The shaded portions represent compounds with good drug properties. A Key to these predictors is presented as footnotes below the table. The assigned asterisk indicates the ligands or complex precursors.

Name	HIA	Aqueous Solubility Level	BBB Level	Hepatotoxicity	Hepatotoxicity Probability[a]	CYP2D6	CYP2D6 Probability[a]	PPB Level	AlogP98 (lipophilicity)	AlogP98 unknown	PSA 2D
TTL3*	3	0	4	1	0.86	1	0.831	2	7.6	0	11.3
TTC3	3	1	4	1	0.841	1	0.613	2	7.4	2	11.3
TTL10*	1	1	0	1	0.668	1	0.891	2	5.9	0	14.7
TTC10[b]	1	1	0	1	0.516	1	0.782	2	5.7	2	14.7
TTL17*	3	1	0	1	0.94	1	0.861	2	7.1	0	12.8
TTC17	2	1	0	1	0.854	1	0.653	2	6.9	2	12.8
TTL24*	0	2	0	1	0.675	1	0.891	2	5.4	0	16.2
TTC24[b]	0	2	0	1	0.523	1	0.782	2	5.2	2	16.2
EK207	3	0	4	1	0.841	0	0.435	2	8.6	6	6.7
EK208	3	1	4	1	0.887	1	0.554	2	7.4	4	6.7
EK219	3	0	4	1	0.953	0	0.475	2	8.5	6	42.4
EK231	3	0	4	1	0.748	0	0.415	2	9.2	6	20.1
MCZS1	0	4	4	0	0.052	0	0.356	0	0.1	2	123.9
MCZS2	0	4	4	0	0.086	0	0.306	0	1.4	2	113.9
MCZS3	1	4	4	0	0.046	0	0.336	0	-1.3	2	120.6
PFK174	3	0	4	1	0.801	0	0.326	2	12.8	4	33.2
PFK189	3	0	4	1	0.774	0	0.198	2	13.7	4	33.2
PFK190	3	0	4	1	0.827	0	0.386	2	15.2	4	33.2
PFK5*	0	4	3	0	0.132	0	0.386	0	1.1	0	73.9
PFK7	0	3	2	1	0.701	0	0.247	0	1.5	5	25.6
PFK6*	0	4	3	0	0.304	0	0.366	0	0.4	0	73.9
PFK8	0	3	2	1	0.86	0	0.108	0	0.8	5	25.6
PFK39*	0	4	3	0	0.384	0	0.079	0	0.3	0	73.9
PFK41	0	4	2	1	0.834	0	0.069	0	0.7	5	25.6
PFK38*	0	4	3	0	0.284	0	0.257	0	0.9	0	73.9
PFK43	0	3	2	1	0.794	0	0.118	0	1.4	5	25.6
KFK154B[b]	0	4	2	1	0.516	0	0.059	0	0.9	2	36.6

Absorption level: 0 = good, 1 = moderate, 2 = low, 3 = very low. **Aqueous Solubility level**: 0 = extremely low, 1 = possible, 2 = low, 3 = good, 4 = optimal. **BBB:** 0 = very high, 2 = medium, 3 = low, 4 = undefined. **Hepatotoxicity:** 0 = non-toxic, 1 = toxic, **CYP:** 0 = non-inhibitor, 1 = inhibitor. **PPB:** 0 = <90% binding, 2 = >95% binding. [a] = probability of occurring, the closer it is to 1 the higher the chance of the compound being hepatotoxic or inhibiting CYP and the closer it is to 0, the higher the probability of the compound not being hepatotoxic or inhibiting CYP. The **PSA** gives an indication of the H-bonding ability and was used together with AlogP98 in determining HIA (shown in Figure 3.7). [b] = 50 /50 chance of being either hepatotoxic or not. AlogP98 unknown represents the number of atoms in the compound with unknown AlogP98.

Table 3.8B: ADMET prediction data for clinically available ARV drugs. The key provided for the descriptors in Table 3.8A also apply here.

HIV drugs	Names	HIA level	Aqueous Solubility level	BBB Level	Hepato-toxicity	CYP 2D6	PPB level	Alog P98	Unknown AlogP98	PSA 2D
NRTIs	Lamivudine	0	4	3	0	0	0	-0.59	0	88.26
	Tenofovir	1	4	4	1	0	0	-0.91	0	133.53
	Emtricitabine	0	4	3	0	0	0	-0.68	0	88.26
	Tipranavir	3	1	4	1	0	2	7.38	0	105.72
	Zalcitabine	0	4	3	0	0	0	-0.99	0	88.26
	Stavudine	0	4	3	1	0	0	-0.32	0	80.51
	Didanosine	0	4	3	1	0	0	-0.84	0	87.79
NNRTIs	Entravirine	2	1	4	1	0	2	5.49	0	116.67
	Nevirapine	0	2	2	1	1	0	2.29	0	55.99
	Delavirdine	0	2	4	0	0	2	2.29	0	110.54
	Efavirenz	0	1	1	0	0	1	4.38	0	39.04
PR	Saquinavir	3	2	4	0	0	0	3.67	0	169.60
	Fosamprenavir	3	2	4	0	0	2	2.54	0	180.33
	Antazanavir	3	2	4	1	0	2	5.08	1	173.73
	Darunavir	2	2	4	0	0	0	2.63	0	142.21
	Ritonavir	2	2	4	1	1	2	5.24	0	145.95
	Amprenavir	1	3	4	0	1	2	2.43	0	133.28
IN	Raltegravir	2	3	4	0	0	0	0.36	0	148.09

The lipophilicity or AlogP98 values which were involved in the model development play a very significant role in determining HIA. According to Kerns and Di, (2008), compounds with ideal lipophilicity values (which should be 0≥3, unlike log P values of <0 [poor lipid bilayer permeability] and >3 [poor aqueous solubility]) also have good solubility patterns. This was observed for the Tscs-based compounds (PFK5, PFK7, PFK6, PFK8, PFK39, PFK41, PFK38 and PFK43), the gold(III) pyrazolyl complex (KFK154b) and two of the gold(I) phosphine thiolate complexes (MCZS1 and MCZS2, Table 3.8A). Compounds TTL10, TTC10 and MCZS3 were predicted to have moderate (1) lipophilicity values with those of TTL10 and TTC10 falling just above the recommended value for “Lipinski’s rule of five” while MCZS3’s value of -1.3 was out of the range indicated by Kerns and Di, (2008).

In Figure 3.7, point plots representing the AlogP98 and PSA ellipses in relation to HIA and BBB penetration for the compounds in this study (Figure 3.7A) and those of currently available ARVs (Figure 3.7B) are shown. Compounds predicted to have good HIA appear within the 95% ellipse (Figure 3.7A) which has an upper PSA limit of 131.4 while those with moderate absorption occupied the 99% absorption ellipse which has an upper PSA limit of 148.12. The poorly absorbed compounds appeared outside both the 95 and 99% ellipses of the AlogP98 versus PSA point plot. The AlogP98 versus PSA point plot for the currently available ARVs is shown in Figure 3.7B. On the list of currently available anti-HIV medication, at least 4 of the 18 compounds (22%) had very low HIA prediction levels (Table 3.8B) and this was mostly the PR inhibitors. This finding suggested that compounds with low absorption could still make it through the discovery process and be useful in a clinical setting. This is

probably because there are exceptions to the rule of five (Walters and Murcko, 2002) making these rules guidelines and not absolute requirements (van de Waterbeemd and Gifford, 2003). The point plots in Figure 3.7 also display BBB penetration ellipses for 95 and 99% confidence levels.

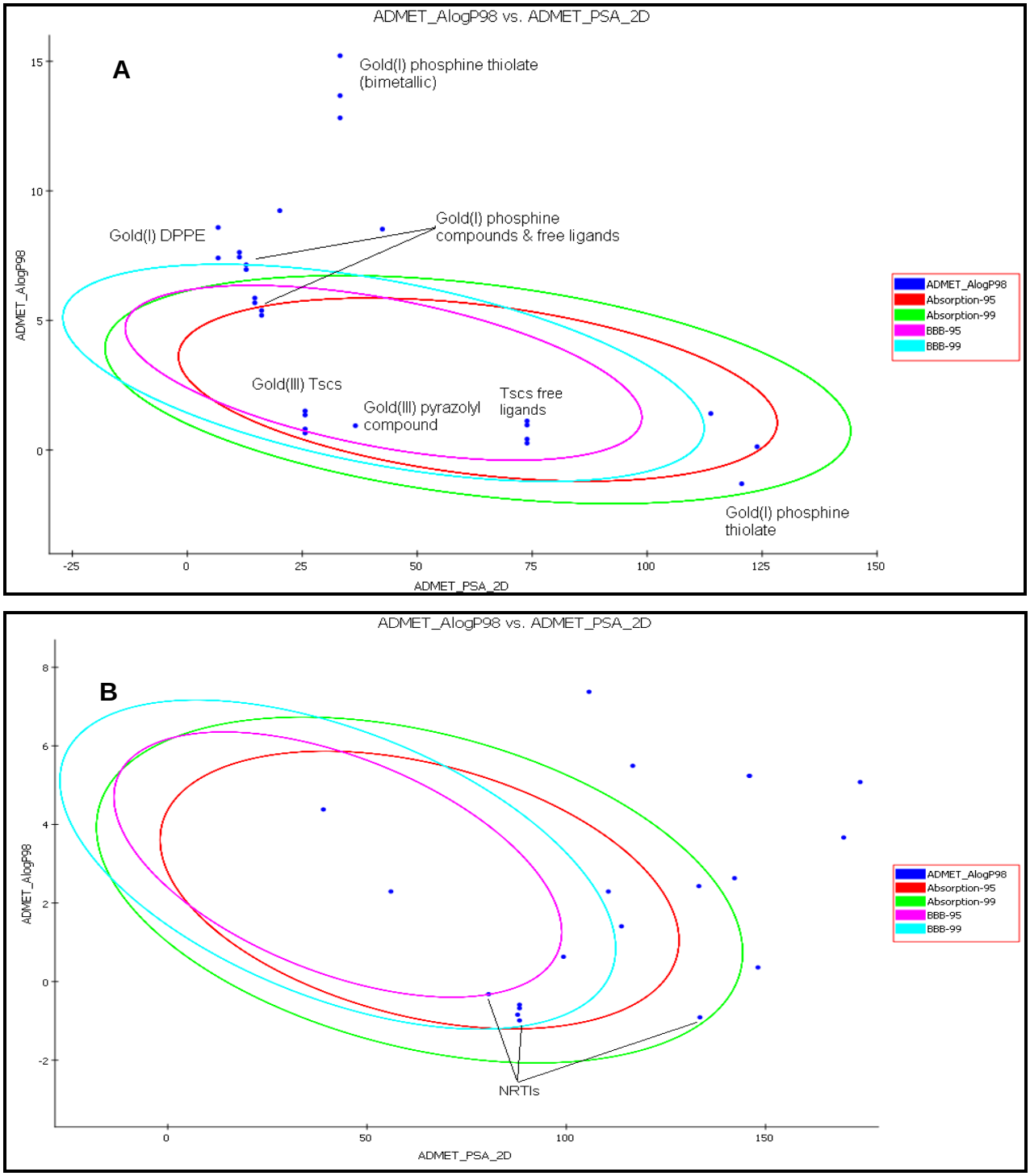

Figure 3.7: Absorption and BBB penetration point plot of the compounds (A) and ARV drugs in the clinic (B). AlogP98 is plotted against PSA. Except for the BPH gold(I) complexes, the gold(I) phosphine bimetallic thiolate complexes and two phosphine chloride compounds (TTL3 and TTC3), the rest of the compounds were predicted to have good HIA levels as they appeared within the 95 and 99% confidence ellipses (A). A total of 18 drugs from the different classes (NNRTIs, NRTIs, PR and IN inhibitors) of ARVs were analysed. Twelve of the drugs were predicted to have acceptable HIA levels and only 8 were predicted to have acceptable BBB penetration levels. A total of 58% of the controls were predicted to be outside the BBB ellipses while at least 37% were outside the HIA ellipses. Each dot on the figure represents a compound. The relative positions of the various classes of compounds are shown in A but only that of the NRTIs (dNTP analogues) in B because there was dispersion within the other groups of ARVs.

3.4.2.2 Prediction of aqueous solubility

Fourteen of the compounds were predicted to have aqueous solubility (25 ºC, pH 7.0) in the drug-like category (Table 3.8A) which includes levels 2, 3 and 4 (Cheng and Merz, 2003). These were TTL24 and TTC24, the Tscs-based compounds (PFK5, PFK6, PFK7, PFK8, PFK38, PFK39, PFK41 and PFK43), the gold(I) phosphine thiolate complexes (MCZS1, MCZS2, MCZS3) and the gold(III) pyrazolyl complex (KFK154b). The rest of the compounds (the gold(I) phosphine chloride complexes and ligands, the BPH complexes, and the three gold(I) phosphine thiolates, PFK174, PFK189, and PFK190) had low to extremely low solubility levels. The extremely low aqueous solubility prediction for PFK174 was not surprising given that this compound was not soluble enough to give a visible ^{31}P NMR peak when the day zero samples were analysed (subsection 3.4.1.3).

It was notable that compounds with ideal aqueous solubility predictions generally had good absorption levels as seen in Table 3.8A i.e. good solubility = good oral absorption (Lipinski *et al*., 1997). In addition, all the compounds with poor aqueous solubility also had very high AlogP98 or lipophilicity values suggesting that these compounds were very hydrophobic. Although attempts were made in increasing the hydrophilicity of the (Au(DPPE)$_2$Cl parent compound in the synthesis of its analogues (EK207, EK208, EK219 and EK231, see section 3.2.2) through the use of nitrogen heteroatoms to replace the lipophilic ethane bridge (Kriel *et al*., 2007), it appears the N bridges were not sufficient in fine tuning the lipophilicity/hydrophilicity. This observation is consistent with findings by Kriel *et al.,* (2007) who noted that the addition of the N bridge in the synthesis of Au(DPPE)$_2$Cl analogues slightly improved selectivity but not sufficiently enough in the targeting of tumour cells over healthy cells. The observed poor aqueous solubility noted for the BPH gold(I) complexes suggested that these compounds would have to be very efficacious for further consideration as drugs and would probably require additional structural modification to improve aqueous solubility.

Only two of the eighteen currently available anti-HIV drugs which were tested as controls (Table 3.8B) had poor aqueous solubility predictions. This observation may be indicative of the importance of aqueous solubility as a drug-like property (Di and Kerns, 2006). Compounds with poor aqueous solubility affect bioassays by causing underestimated activity, reduced HTS hit rates, result in variable data, inaccurate SAR, discrepancies between enzyme and cell assays and inaccurate *in vitro* ADMET testing (Di and Kerns, 2006). While aqueous solubility is a required property, it is important that a balance be obtained because very high aqueous solubility which is usually associated with poor lipophilicity means compounds with such properties cannot be orally available.

3.4.2.3 Prediction of blood brain barrier penetration

Three of the phosphine ligands and corresponding gold(I) complexes (TTL10, TTC10, TTL17, TTC17, TTL24 and TTC24) were predicted to have very high BBB penetration levels

(0), while the thiosemicarbazonate gold(III) complexes (PFK7, PFK8, PFK41 and PFK43) and the gold(III) pyrazolyl complex (KFK154b) had medium BBB penetration prediction levels of 2 (Table 3.8A). The Tscs ligands PFK5, PFK6, PFK39 and PFK38 had moderate BBB penetration. Complexation with gold appeared to improve BBB penetration for the complementary complexes. The rest of the compounds i.e. TTL3 and TTC3 from the phosphine chloride class, the BPH gold(I) complexes and the gold(I) phosphine thiolate complexes were predicted as having undefined (ranked 4) BBB penetration levels. These compounds also appeared outside the 99% ellipse (seen in Figure 3.7) while those with acceptable penetration levels were within the 95 and 99% confidence ellipses for BBB penetration. BBB penetration is important for anti-HIV agents to be able to combat infection and inhibit viral replication in the brain (Glynn and Yazdanian, 1998). Existing anti-HIV agents such as nevirapine are able to cross the BBB (this ability is attributed to its lipophilicity, Glynn and Yazdanian 1998). According to the predictions that were performed for the current anti-HIV drugs (Table 3.8B and Figure 3.7B), nevirapine had a BBB level of 2 (medium penetration) supporting the findings by Glynn and Yazdanian (1998). The majority of the HIV drugs either had low or undefined BBB penetration levels (Table 3.8B and Figure 3.7B) especially the PR inhibitors, a finding which has been confirmed by other authors (Enting *et al*., 1998). This suggests that these drugs would be unable to arrest or reduce viral replication in the brain, a situation that has been shown to result in increased incidence of AIDS dementia (Marra and Booss, 2000). Except for TTL3 and TTC3, the phosphine chloride compounds (TTL10, TTC10, TTL17, TTC17, TTL24 and TTC24), the gold(III) thiosemicarbazonate complexes (PFK7, PFK8, PFK41 and PFK43) and the gold(III) pyrazolyl complex (KFK154b) could be better inhibitors of HIV replication in the brain (BBB levels of 0 = very high and 2 = medium). While good BBB penetration predictions were observed for the phosphine chloride compounds (ligands and complexes), unfortunately aqueous solubility was very poor (except for TTL24 and TTC24). These compounds will therefore require further structural modification to fine tune lipophilicity/hydrophobicity so as to obtain ideal lipophilicity values. This observation confirms the ideology that finding a perfect drug is not easily achievable in drug discovery (Joshi, 2007).

3.4.2.4 Prediction of cytochrome P450 2D6 inhibition

Except for the phosphine chloride compounds of class I (Table 3.6) and the BPH gold(I) complex (EK208) which were predicted to be CYP inhibitors, none of the other compounds had such effects (Table 3.8A). This finding is promising for these compounds because inhibition of CYP is not desirable. CYP is involved in drug metabolism (Susnow and Dixon, 2003) and its inhibition could potentially block the metabolism of other drugs. Anti-HIV drugs are administered in combination and if one of the drugs is a CYP inhibitor, its metabolism and that of the other drugs will be compromised. This can lead to a reduction in bioavailability

resulting in enhanced mutation rate since suboptimal doses will end up in the circulation. Alternatively it could result in interactions that may lead to elevated blood levels of some of the drugs that are used such that unwanted and life-threatening side effects could ensue (Tanaka, 1998). Only three of the eighteen anti-HIV drugs for which ADMET predictions were determined had the potential of inhibiting CYP. These included the NNRTI, nevirapine and two PR inhibitors (ritonavir and amprenavir, Table 3.8B).

3.4.2.5 Prediction of hepatotoxicity

Hepatotoxicity prediction levels according to the ADMET protocol could either be 1= hepatotoxic, or 0 = non hepatotoxic. This ranking is further classified based on the likelihood of the toxicity occurring and represented by probability values (Table 3.8A). The closer the probability is to one, the higher the likelihood of the compound being hepatotoxic and the closer to zero, the higher the likelihood of it being non hepatotoxic. The phosphine compounds (TTL10, TTC10, TTL24 and TTC24), the gold(I) phosphine thiolate complexes (MCZS1, MCZS2 and MCZS3) and the Tscs ligands (PFK5, PFK6, PFK38 and PFK39) were predicted as non hepatotoxic (0). The rest of the compounds were hepatotoxic. The gold(III) pyrazolyl complex (KFK154b) was predicted as hepatotoxic but with a 0.516 probability (Table 3.8A). Eight of the eighteen anti-HIV medications on the control list (Table 3.8B) were predicted to be hepatotoxic. Although being hepatotoxic is not a drug-like property, because it can be clinically managed through physician intervention (Núñez, 2010), efficacious drugs with this property can make it through the drug discovery process and be clinically useful e.g. nevirapine in Table 3.8B.

3.4.2.6 Prediction of plasma protein binding ability

Eight gold complexes had a <90% chance of binding to plasma proteins. These were the gold(I) phosphine thiolate complexes, MCZS1, MCZS2 and MCZS2, the gold(III) thiosemicarbazonate complexes and complementary ligands (Table 3.4) and the gold(III) pyrazolyl complex (Table 3.5) with a classification of 0. This classification which also makes use of AlogP98 groups such compounds as having an AlogP98 of <4 (Table 3.8A). The gold(I) phosphine chloride complexes and free ligands (class I) and the BPH complexes (class II) as well as the gold(I) phosphine thiolate bimetallic complexes (PFK174, PFK189, PFK190) of class III on the other hand were predicted as having a > 95% chance of binding to plasma proteins and AlogP98>4. Compounds with a <90% chance of binding to plasma proteins, are more drug-like because the free drug will be able to stay in solution for penetration into tissue and will thus be able to reach the therapeutic target (Kerns and Di, 2008). Binding to plasma proteins tends to affect the concentration of a compound in bioassays involving the use of reagents such as fetal calf serum (FCS) and this could drastically affect *in vitro* efficacy (Lin *et al*., 2008, Kageyama *et al*., 1994). Compounds (e.g. those in class I, II and the three bimetallic

complexes of class III) with high PPB binding tendencies that inhibit in direct enzyme assays will have an increased likelihood of complete loss of activity in cell-based assays and *in vivo* (Kageyama *et al*., 1994).

3.4.2 7 Drug-likeness summary for the compounds

Seven properties i.e. the six ADMET descriptors (HIA, aqueous solubility, BBB penetration, hepatotoxicity, PPB binding and CYP inhibition) and lipophilicity predictions were obtained for each of the twenty seven compounds in this study. These properties were used to construct an in-house drug score table (Table 3.9). According to the summary, only one gold complex (KFK154b) was predicted as having favourable properties for all ADMET descriptors (although with a 50% chance of being hepatotoxic) while seven complexes were positive for 6 out of 7 descriptors. Complex TTC24 and complementary ligand TTL24 had a score of 3 out of 7 with TTC24 having a 50% chance of being hepatotoxic. The least drug-like compounds were TTC3, its free ligand TTL3 and the BPH gold(I) complex EK208. With regards to classes, drug-like characteristics were common for three complexes from class III (MCZS1, MCZS2 and MCZS3), four from class IV (PFK7, PFK8, PFK41 and PFK43) and one from V (KFK154b). The predicted properties were similar when literature comparisons were made with those of the anti-arthritic gold complex, auranofin (also included here as MCZS2).

With regards to functional groups, the ligands played a very important role in the ADMET rankings for each class of compounds. For example, all the phosphine containing compounds which also had phenyl rings had significantly higher AlogP98 values (due to the hydrophobicity related to these rings) than the gold(I) phosphine thiolate complexes (MCZS1, MCZS2 and MCZS3) which have glucose rings and more H-bond acceptors and were less hydrophobic. The Tscs ligands of class IV (Table 3.4) which contain more H-bond donors (Table 3.6) tended to be less lipophilic (than the phosphine group of ligands) while the corresponding gold complexes (Table 3.4) had slightly higher but ideal values (Table 3.8A). The slightly higher values probably resulted from the fact that there was a decrease in the number of H-bond donors after complexation as seen in Table 3.6 where the free ligands had 4 H-donors and upon complexation only 2 were available. Some complexes e.g. the thiosemicarbazonate complexes had better drug-like predictions than some currently available anti-HIV agents e.g. nevirapine (Table 3.8B). Nevirapine has the potential of inhibiting CYP which is not the case for eighteen of the 27 compounds in this study. A look at Table 3.9 also suggests that drug-like properties for the complexes were usually similar to those of the ligand precursors e.g. TTL3 and TTC3 which had a total score of 1 and the Tscs ligands and complexes a score of 6/7. The Tscs compounds, the gold(III) pyrazolyl compound and the gold(I) phosphine thiolate compounds containing 2,3,4,6-tetra-O-acetyl-1-thio-B-D-glucopyranose were the most drug-like.

Table 3.9: ADMET prediction scores summary. Compounds with a score of 0/7 were those predicted to be the least drug-like while those with a score of 6/7 were those predicted to be the most drug-like. Ligand precursors and corresponding complexes from different classes had similar scores suggesting that drug-likeness was related to ligand type.

Drug Score/7	Gold complex(s)		Free ligand(s)
	Gold(I)	Gold(III)	
0	TTC3, EK208		TTL3
1	TTC17 EK207, EK219, EK231, PFK174 PFK189, PFK190		TTL17
2	TTC10		TTL10
3	TTC24		TTL24
6	MCZS1, MCZS2 and MCZS3	PFK7, PFK8, PFK41 and PFK43, KFK154b	PFK5, PFK6, PFK39 and PFK38

3.4.3 Shake Flask Method of Lipophilicity Determination

In addition to using the DS® Client software package for predicting AlogP98 (lipophilicity) and its relation to other drug-like properties, lipophilicity determination was also done for gold complexes PFK7 and PFK8 using the traditional shake flask method. This method entails determining the concentration of the compounds in an aqueous and a lipid phase followed by calculating the logarithm of the partition coefficient (Log P) between the phases as a measure of lipophilicity. **Log P** values of **2.42±0.6** and **0.97±0.5** were obtained for complexes PFK7 and PFK8 respectively.

The slight differences between log P values obtained by the shake flask method and those from DS® (which were 1.5 and 0.8 for PFK7 and PFK8 respectively) might be as a result of the presence of the gold atom in the complexes. These atoms are not included in the ADMET AlogP98 protocol in DS®, because the program was designed from datasets involving organic molecules. This leads to 5 atoms (making the coordination sphere) for the gold(III) thiosemicarbazonate complexes (PFK7, PFK8 - Table 3.4) and all the gold complexes to have unknown AlogP98 values (Table 3.8A). Atoms with unknown AlogP98 do not contribute to the AlogP98 calculation. However, this did not seem to have had a drastic effect on the AlogP predictions from DS® when compared to those from the shake flask method since very similar values were obtained. This observation was further supported by the fact that ideal lipophilicity predictions were obtained for auranofin which is a known orally available gold-based drug as a result of its lipophilic ability.

3.5 CONCLUSIONS

ADMET properties are required early on in drug discovery to help with prioritising lead compounds and for reducing late failures. While *in vitro* HTS methods can be implemented, *in silic*o predictions (which are easily obtained) can serve as complementary approaches for substantiating the *in vitro* findings. In addition to using Discovery Studio for predicting ADMET parameters for the compounds in this study, NMR was also used for determining the stability

of representative complexes in *d6*-DMSO after storage at two different temperatures (-20 and 37 ºC).

Backbone chemical shifts of the complexes generally appeared stable after storage at -20 and 37 ºC as seen from ^{31}P and ^{1}H NMR spectra. The main changes appeared to be impurities such as acetone (spectrum of EK231) and D_2O peak in the ^{1}H spectrum of KFK154b. Another notable change was that of inherent hygroscopic abilities of four complexes while the ^{31}P and ^{1}H NMR spectra of MCZS3 and PFK174 could not be resolved because of poor solubility in DMSO (Table 3.7) stemming from the presence of water which is known to lead to compound precipitation when in DMSO (Ellson *et al*., 2005).

With regards to drug-likeness predictions, twelve of the compounds (classes III, IV and V) had a score of 6 out of 7 (Table 3.9) which correspond with literature reports for auranofin (MCZS2), a clinically and orally available gold(I) complex that has been reported to restore the CD4+ count of an AIDS patient who was being treated for psoriatic arthritis (Shapiro and Masci, 1996). This compound was predicted to have ideal lipophilicity and HIA values. BBB penetration predictions for nevirapine also correlated with the experimentally determined findings of Glynn and Yazdanian (1997).

Another notable observation was the fact that ADMET properties, as expected, were dependent on the groups present in the compounds. For example the *N,N*-dimethly-ethane-1,2-diamine moiety present in TTC10 and TTC24 appeared to confer better drug-like properties unlike the phenethyl-amine group present at a similar position in TTC3 and TTC17 (all complexes belonging to class I).

While some of the compounds were predicted as having favourable ADMET and Lipinski's properties, it should be noted that these are not absolute requirements and that there are exceptions that do go through to clinical application. For these reasons, where possible, all the compounds synthesised in this study were analysed in anti-HIV tests and the calculated/determined predictions here were not stringently used to filter out non drug-like compounds. The anticipation was that efficacious compounds with poor ADMET predictions could eventually be recommended for structural modifications through SAR studies to increase drug-likeness while maintaining therapeutic usefulness. Those with good drug-like properties on the other hand, which end up having therapeutic efficacy would be recommended for further testing.

Confirmatory tests between methods (*in silico* and shake flask for complexes PFK7 and PFK8) and with literature (for auranofin) suggested that the inorganic nature of the compounds did not seem to drastically affect ADMET predictions which were obtained from software that was developed for organic compounds (Fricker, 2007). The ADMET predictions of PFK7, PFK8 and the rest of the Tscs-based complexes and the shake flask findings form part of a publication from this project (Fonteh *et al*., 2011).

Finding an ideal drug (based on *in silico* and experimental data) is always desirable, but not always possible (Joshi, 2007) as seen from the data for the currently available anti-HIV agents. What is important therefore is obtaining a balance with regards to efficacy and tolerability while ensuring appropriate physician intervention protocols at the point of administration.